Vol. 25(3S):399-408 | Ocean and Polar Research | December 2003

Article

Behavior of Currents and Suspended Sediments around a Silt Screen

Jae-Youll Jin[1]*, Jang Won Chae[1], Won Oh Song[1], Jin Soon Park[1], Sung Eun Kim[1], Weon Mu Jeong[1], Ki Dai Yum[1], and Jae Kyung Oh[2]

[1]*Coastal and Harbor Engineering Research Division, KORDI*
Ansan P.O. Box 29, Seoul 425-600, Korea
[2]*Department of Oceangraphy, Inha University*
Incheon 402-751, Korea

Abstract : The behavior of Suspended Sediment Concentrations (SSC) around a silt screen in a microtidal coastal area was hydrodynamically measured. The current speed at the mid-layer about 30 m downstream of the screen reduces to about half that at the same distance upstream. It was caused by the contraction of the vertical section due to the screen. Even during a relatively weak storm period, the SSC increases to that of the value caused by dredging. Section-averaged SSC at the downstream of the screen is higher by about 60% than that at the upstream, suggesting that the silt screen plays an adverse effect rather than a constructive role in the reduction of SSC generated by dredging.

Key words : silt screen, microtidal, Optical Backscattering Sensor (OBS), acoustic velocimeter, mitigation, sediment plume, sediment flux

1. Introduction

Sediment plumes arising from various coastal works can cause detrimental effects on the coastal ecosystem in various ways. Although the most active countermeasure against the plumes is to restrict the works to specified time periods known as *environmental windows* (Reine *et al.* 1998), silt screens have been widely used for reducing the spread of artificially generated suspended sediments (SS).

However, it has been recognized that the performance of a silt screen is quite sensitive to primary conditions, including bottom sediment, current speed, wave height, dredger type, etc., which means that if not carefully designed and applied, the screen will disturb the seafloor and cause sediment resuspension (Ooms 1997). Hence, the use of silt screens is not always practical or economic, and expert attention is needed during their design and use. Thus, it may be desirable to carry out a pilot test as was made in the Penny Bay Development in Hong Kong (Mouchel Asia Ltd. 2002) to check whether the silt screen achieves the expected performance especially in construction projects of long-term and large dimensions.

However, Korean regulators have requested the use of silt screens in almost all coastal works without a quantitative consideration of their efficiency and any potential increase of SSC.

In order to assess the mitigation efficiency of a traditional silt screen of a fixed hanging type, intensive field measurements were carried out in the area of Busan New Port, which is being constructed, corresponding with located at the southeastern tip of Korea.

2. Field measurements

The coastal area around Busan New Port, where a great excavation project spanning 63.6 million m^3 has being dredged for the construction, is shown in Fig. 1. During the working period of three mechanical dredgers (Table 1) in the study area shown in Fig. 1, field measurements were carried out to assess the efficiency of the silt screen (Fig. 2).

*Corresponding author. E-mail : jyjin@kordi.re.kr

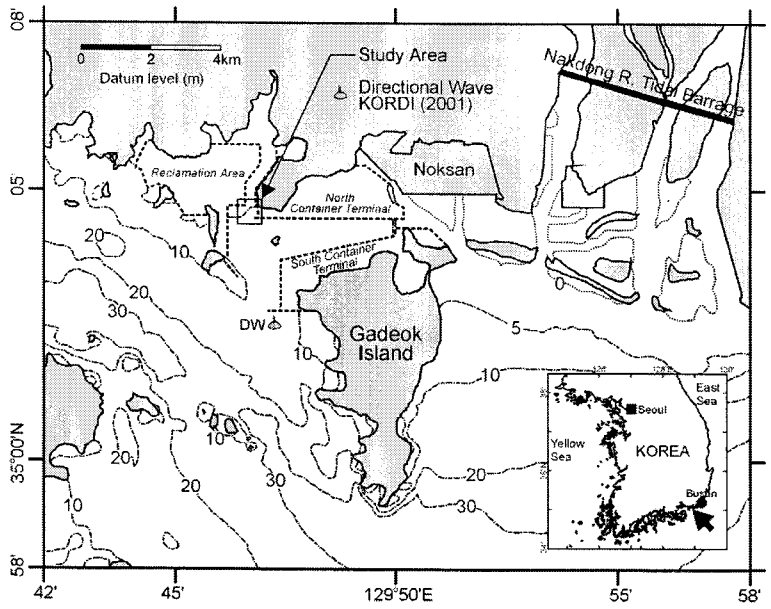

Fig. 1. Location map of Busan New Port under construction and the study area.

Table 1. Working periods and dredged volumes of target dredgers.

Period	Dredger	Dredged Volume (m^3)
08:00-20:00 July 5	Backhoe (3.5 m^3)	1,000
08:00-14:00 July 6	Backhoe (3.5 m^3)	500
07:00-18:00 July 8	Backhoe (3.5 m^3)	500
07:00-18:00	Grab (4 m^3)	500
04:00-24:00	Grab (8 m^3)	2,000
07:00-18:00 July 9	Backhoe (3.5 m^3)	500
07:00-18:00	Grab (4 m^3)	500
04:00-24:00	Grab (8 m^3)	2,000
07:00-18:00 July 10	Backhoe (3.5 m^3)	500
07:00-18:00	Grab (4 m^3)	500
04:00-24:00	Grab (8 m^3)	1,500
07:00-18:00 July 11	Backhoe (3.5 m^3)	500
07:00-18:00	Grab (4 m^3)	500
07:00-18:00 July 12	Grab (4 m^3)	500

The work area of each dredger was approximately 20 m and 110 m, respectively in longitudinal and latitudinal directions. At a distance of 220 m to 330 m southward from the dredgers, silt screens of a fixed hanging type had been installed. The vertical screen length and water depths were approximately 3 m and 5.5 m, respectively. The spring rise at the Gadeok Tidal Station near the study area is 1.8 m.

Bottom sediment was sampled at 23 positions (Fig. 2). Time series observations of SSC, water depth, current velocity, and direction at 3 m above the bed (mab) of site A1 (July 5-8, 2001) and A2 (July 5-11, 2001) were made every five minutes with sediment flux monitoring systems (AURYs) consisting of 8 automatic water samplers of Auttles (Jin *et al.* 2003), a multi-parameter monitor of YSI6600, and current meter of RCM9.

A benthic boundary layer monitoring system, SPHINX (KORDI 2000), deployed at site S, measured current velocity and optical turbidity at 25, 30, and 50 cm above the bed (cmab), as well as wave characteristics with acoustic velocimenters (VECTORs), a wave-current recorder (AWAC) of Nortek, and optical backscattering sensors (OBS-3s) of D&A Instrument Co. from July 7 to 11, 2001.

Additionally, SSC profiles were measured at 6 sites 1-1 to 2-3 with a YSI6600 in an ebb dredging period lasting about 4 hours on July 10, 2001.

3. Results

Bottom sediments

Particle compositions and the statistical parameters from the 23 sites are presented in Table 2. The mean diameters (d_m) are generally about 5ϕ (31.3 μm) to 6ϕ (15.6 μm). The difference of d_m at B17 and B21 may result in a difference of SSC at A1 and A2 to some degree. The standard deviations (σ) ranging from 2 to 4ϕ mean that the bed materials are very poorly sorted.

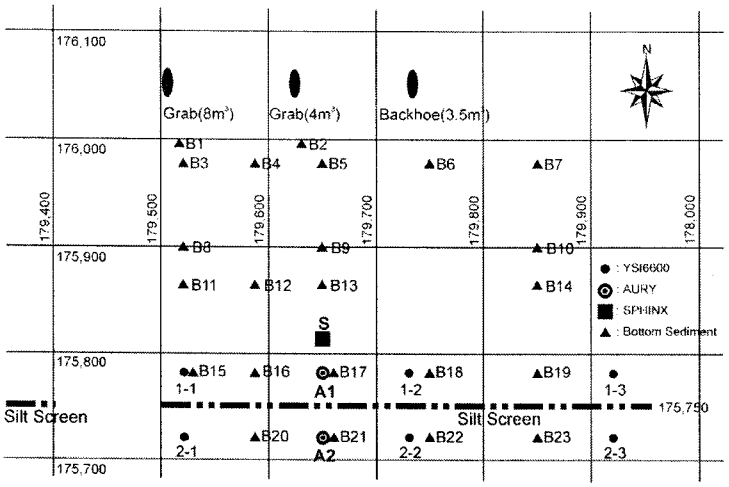

Fig. 2. Location map of field measurements in TM coordinates.

Table 2. Particle composition of bottom sediments and the statistical parameters by moment method.

Station B#	Weight composition (%)				d_m (ϕ)	σ (ϕ)	S_k	K_t
	Gravel	Sand	Silt	Clay				
1	1.3	23.1	53.9	21.6	5.7	2.8	−0.5	2.6
2	4.6	27.2	46.8	21.5	5.2	3.3	−0.4	2.2
3	1.0	31.7	50.8	16.5	5.3	2.7	−0.1	2.5
4	18.7	41.4	29.5	10.4	2.9	3.7	0.2	1.9
5	0.0	15.8	59.8	24.5	6.3	2.3	−0.3	2.8
6	0.1	41.8	46.9	11.2	4.8	2.3	0.6	3.1
7	4.9	24.3	52.6	18.3	5.2	3.1	−0.5	2.8
8	0.2	15.3	62.7	21.7	6.4	2.1	−0.3	3.0
9	0.0	32.9	54.2	12.9	5.2	2.2	0.6	2.7
10	2.1	36.2	46.9	14.8	4.7	3.1	−0.1	2.1
11	0.0	17.1	62.1	20.9	6.1	2.2	0.0	2.7
12	4.0	24.0	51.7	20.3	5.4	3.1	−0.5	2.5
13	0.0	40.6	47.4	12.0	4.8	2.5	0.2	2.7
14	0.7	29.8	55.2	14.2	5.2	2.4	0.2	2.9
15	0.0	19.7	60.2	20.1	6.0	2.2	0.2	2.4
16	0.0	23.3	57.9	18.8	5.8	2.4	−0.1	2.7
17	1.3	60.2	33.2	5.3	3.9	2.0	0.8	5.1
18	2.3	44.1	39.8	13.8	4.3	3.2	0.1	1.9
19	4.6	59.8	26.5	9.1	3.1	3.2	0.6	2.3
20	4.9	38.5	45.9	10.8	4.5	2.7	−0.2	3.6
21	0.0	16.6	60.7	22.8	6.1	2.5	−0.4	3.0
22	1.2	35.1	49.0	14.7	5.0	2.6	0.1	2.7
23	0.0	12.4	63.9	23.7	6.4	2.1	−0.1	2.7

Tidal currents and SSC

After in-situ calibration of the OBS turbidity in nephelometric turbidity unit (NTU) with SSC in the seawater concurrently sampled by the Auttles (Fig. 3), temporal variations in current speed, current direction, and SSC at 3 mab of sites A1 and A2 are shown in Fig. 4. Fig. 4(b) shows the data of only A2 because the AURY at A1 was retrieved on July 8.

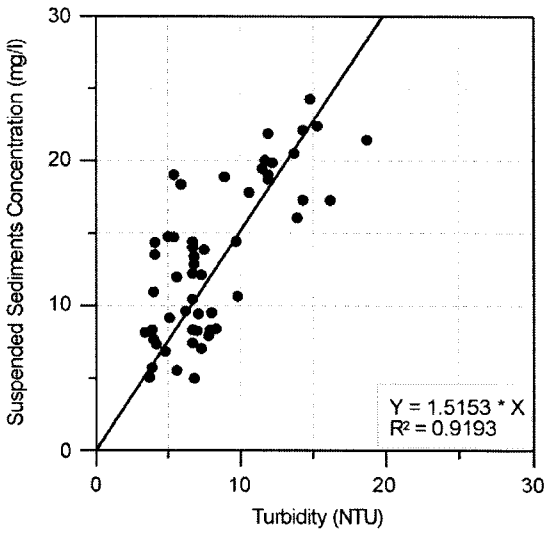

Fig. 3. Correlation between OBS turbidity and SSC.

Maximum speeds of northward flood currents at A1 and A2 are about 25 cm/s and 40 cm/s, respectively, while those of southward ebb currents are about 40 cm/s and 25 cm/s. This suggests that the current speed of the mid-layar becomes weaker across the screen. Considering the relatively short distance of about 60 m between A1 and A2, these temporal variations may be caused by the screen rather than by local bathymetric characteristics.

SSC varies from about 5 to 90 mg/*l*. Dredging-induced

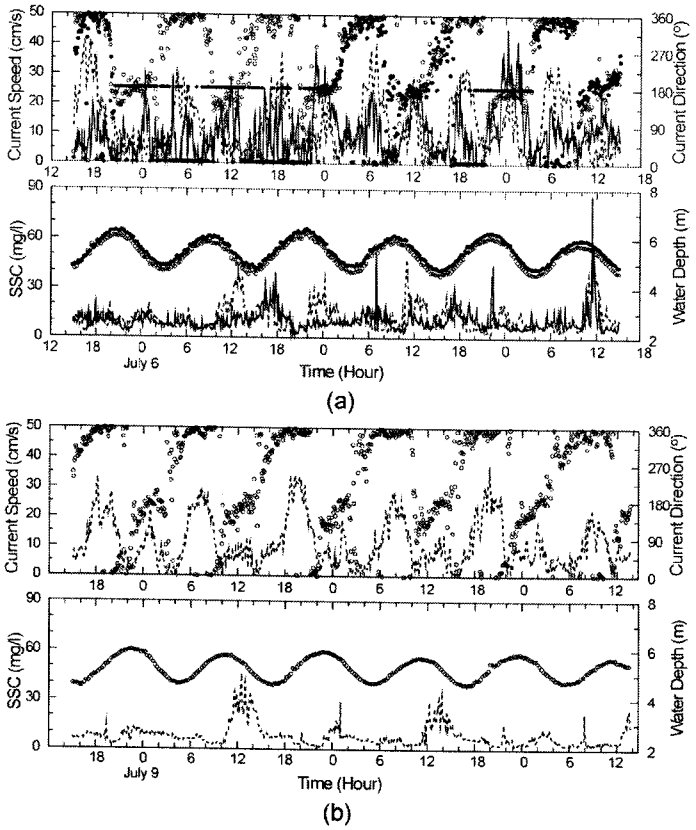

Fig. 4. Results of AURY monitoring at mid-layers of sites A1 and A2; heavy (A1) and open (A2) circles are current direction and water depth, solid (A1) and dotted (A2) lines are current speed and SSC, respectively. The lower panel (b) shows the data only at site A2.

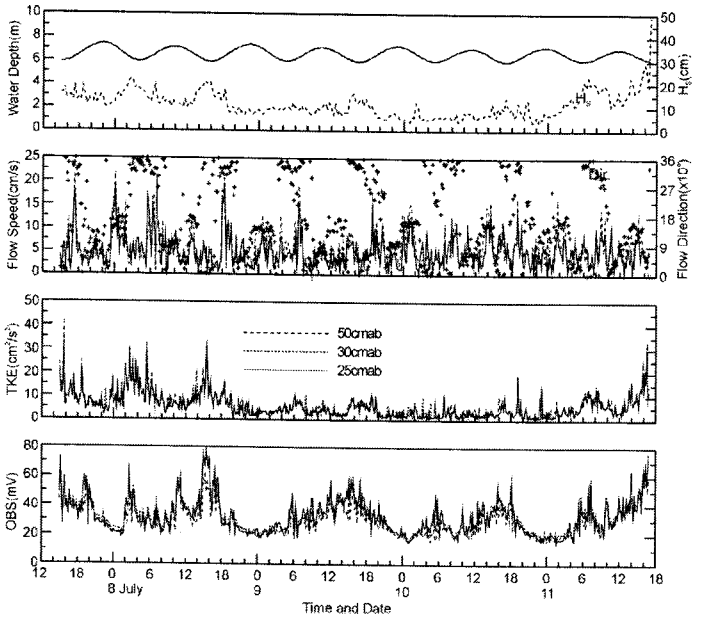

Fig. 5. Temporal variations of hydrodynamic parameters and OBS voltage at 3 near-bed layers at site S. TKE=Turbulent Kinetic Energy.

plumes can directly influence the SSC at A1 and A2 only during the ebb period. Thus, it is apparent that the background SSC around the study area ranges from 5 to 20 mg/*l*, recorded until 08:00 July 6, during which only the backhoe dredger was working during the flood tide (Fig. 4).

In comparison, from 09:00 on July 6 to 04:00 on July 8, the peaks occurred even during flood tides. Furthermore, SSC at A2 located farther from the dredging sites is higher than that at A1 during the ebb period. Neither dredging operations nor normal conditions without dredging can explain these abnormally high SSCs, especially on July 7 when none of the dredgers worked. Hence, more detailed discussions are required.

It is believed that the SSC peaks in ebb periods after about 10:00 on July 8 reflect the sediment plumes generated by the dredging. SSC at A1 increases up to about 90 mg/*l* during the last ebb period in Fig. 4(a) when all the 3 dredgers were working, while the corresponding peak at A2 is about 40 mg/*l*. A sudden drop in the SSC at A2 at about 01:00 on July 10 during the ebb period seems to be due to the termination of the 8 m^3 dredger's single task.

Currents and OBS voltage at 3 near-bed layers of site S measured with the SPHINX are shown in Fig. 5 with water depth, significant wave height, and turbulent kinetic energy (TKE) computed with 3-dimensional current velocimeters of 8 Hz:

The magnitudes of current speeds at 25, 30, and 50 cmab are about the same, the maximum of which is about 20 cm/s. Although the distance between sites S and A1 was only about 30 m, most of the flood peaks at site S are considerably higher than the ebb ones, a reversing phenomenon to the ebb-dominated regime observed at site A1.

The magnitudes of OBS voltages in the three layers are also more ore less similar with slightly higher values at the lowest layer (Fig. 5). Unfortunately, the OBSs were not calibrated in situ. However, assuming that the size distribution of suspended particles at S is similar to that of A1, and then applying the manufacturer's calibration result relating 5 volts to 2,000 NTU, and the correlation formula in Fig. 3, the minimum of 20 mV and the maximum of 80 mV in Fig. 5 can be related to 12 mg/*l* and 50 mg/*l*, respectively. Given the minimum SSC at sites A1 and A2, the results of this indirect calibration seem to be reasonable. In this estimation, however, it should be noted that the OBS gain (volts per mg/*l*) varies by a factor of up to 200 according to particle size (D&A Inststrument Company 1991).

In the period from about 04:00 on July 8 to 24:00 on July 10, the OBS turbidity in voltage varies dramatically according to dredging operation and tidal phase. The major peaks were associated with the ebb period when all the dredgers were working. During the remaining period, however, OBS turbidity has a closer relationship with TKE, which means the substantial effects of waves.

SSC profiles at the paired front and rear sites during the ebb period are shown in Fig. 6. Although there are some

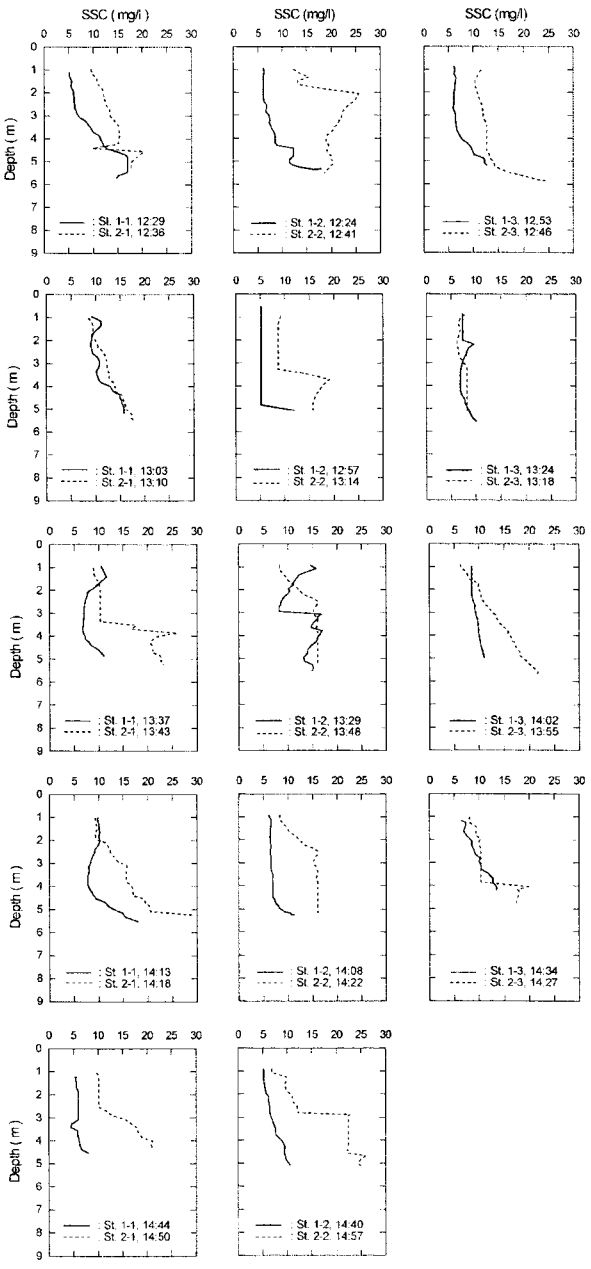

Fig. 6. SSC profiles at the paired front and rear sites of the silt screen on July 10, 2001.

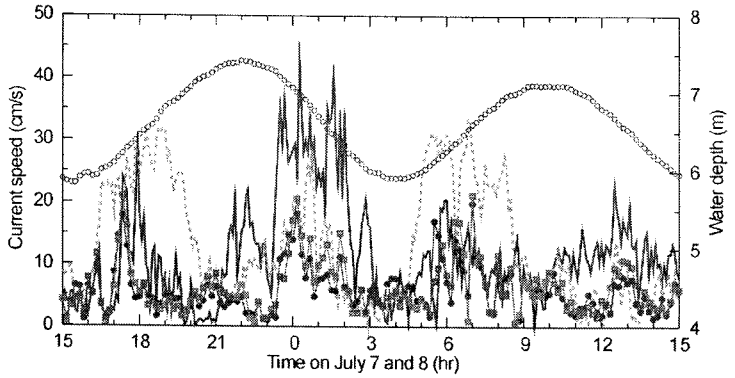

Fig. 7. Temporal variations of current speeds at 3 mab of sites A1 (blue bold solid line) and A2 (green bold dotted), at 25 cmab (blue line with filled circles) and 50 cmab (red with open square) of site S. Open circles represent water depth at S.

time gaps of 5 to 14 minutes between the paired profiles due to unsynchronized monitoring, it must be noted that most of the SSCs at the downstream sites 2-1, 2-2 and 2-3 are considerably higher than those upstream. Additionally, the vertical gradients of SSC in shallower and deeper zones than 3 m of screen depth are markedly distinguished, especially downstream, which most likely results from resuspension of bottom sediment near the silt screen. Averages of the depth-averaged SSC at the upstream and downstream sites are about 8.9 mg/*l* and 14.2 mg/*l*, respectively.

According to the results presented above, it is necessary to discuss the relative magnitudes of current speeds at sites A1, A2 and S, generation of SSC peaks, and the possible influence of the screen on related processes.

4. Discussion

Influence of the silt screen on current and suspended sediment concentrations

Temporal variations of current speeds at sites A1, A2 and S over 24 hours are shown in Fig. 7 with the tidal curve at S. The relative magnitudes of current speed according to tidal phase are shown in Table 3. Current speed at A2 is higher than that at A1 by about 10 cm/s during the food period, while vice versa during the ebb period. Near-bed speeds at S are comparable to the speed at 3 mab of A1 during flood tides and A2 during the ebb period, respectively. Assuming that current velocity near the bed of A1 is similar to those at S, the vertical gradient upstream is steeper than downstream.

The characteristics of these relative magnitudes is believed to be caused by the silt screen. The conceptual drawing of the related processes is shown in Fig. 8. As

Table 3. Tidal phase-averaged current speeds.

Tidal Phase	Phase-averaged Current Speed (cm/s)				
	S			A1	A2
	25cmab	35cmab	50cmab	3mab	3mab
Flood I	5.23	5.33	5.74	7.59	16.68
Flood II	6.93	7.02	6.99	9.03	18.32
Flood Averaged	6.08	6.17	6.36	8.31	17.50
Ebb I	6.44	6.76	7.09	19.50	9.85
Ebb II	4.01	4.17	4.89	11.80	5.41
Ebb Averaged	5.23	5.46	5.99	15.65	7.63

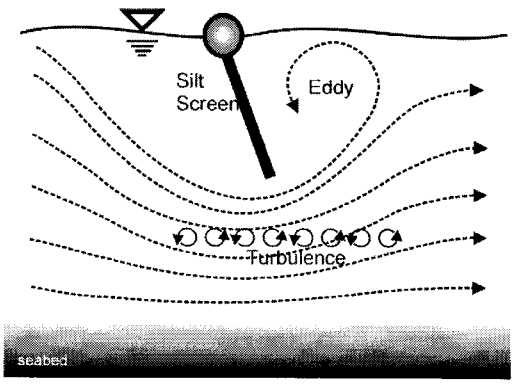

Fig. 8. Conceptual drawing of current fields near a silt screen.

seawater passes through the contracted section (CS) between the screen bottom and the seabed, it accelerates. Turbulence intensity near the CS should be enhanced and eddies of considerable size may be generated in the rear of the section. Hence, the current speed and profile at the downstream feeling the CS effect could be largely different from that upstream at the same distance.

In this context, it is unlikely that suspended sediments

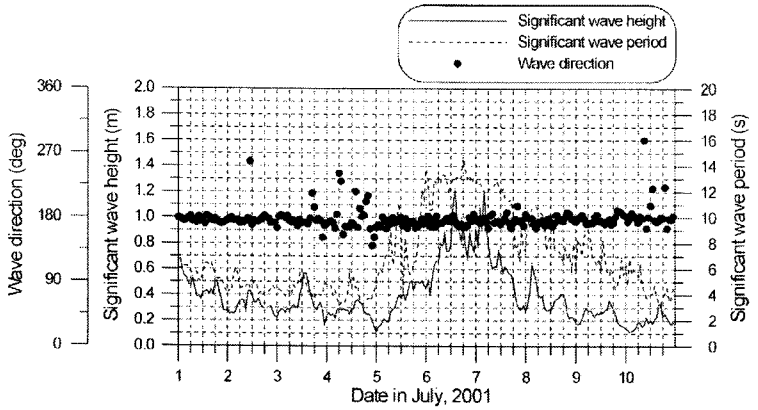

Fig. 9. Wave characteristics at DW (KORDI 2001).

in the CS have settled considerably. Furthermore, an improper installation designed of a silt screen can cause erosion of the seabed, which should be at its worst if the bed is highly contaminated. Stepwise sudden increases of SSC just downstream of the screen shown in Fig. 6 presumably result from the CS effect and hence some erosion of the seabed. In fact, the silt curtain in the study area plays an adverse effect by 60%, judging from the averages of depth-averaged SSCs rather than SS fluxes.

However, the increase in SSC downstream does not mean an increase in SS flux. Considering the relative magnitudes of current speeds at A1 and A2, the fluxes may be comparable.

SSC near the silt screen in storm periods

The SSC peaks in the period without any dredging activity (09:00 on July 6 to 04:00 on July 8) may be associated with comparatively rough wave condition. Since 1999, the KORDI has been monitoring wave characteristics at site DW 4 km southward from the silt screen. The wave characteristics (Fig. 9) indicate that the SSC peaks from July 6 to 7 were generated by increasing bed shear stress.

Correlation between significant wave heights measured by a directional waverider buoy at site DW and those by a pressure gauge at site S is shown in Fig. 10, some deviations in which might be due to locally generated short-period waves.

Wave height at A1 can be evaluated by the equation in Fig. 10 because site S is just 30 m northward from A1. If the silt screen causes wave damping, wave height at A2 may be higher than that at A1. However, according to the experiments of Bruun (1989) shown in Fig. 11, a total of about 90% of incident wave energy is transmitted through the opening of the screen, where the screen depth is half

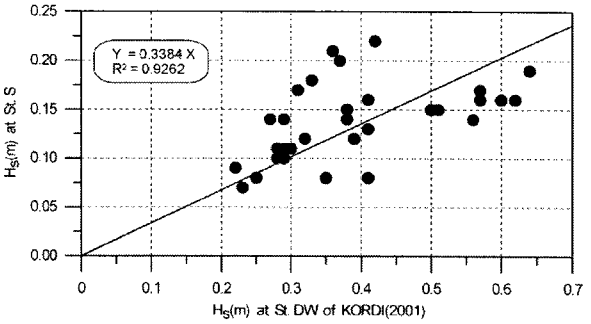

Fig. 10. Correlation between significant wave heights at sites DW and S.

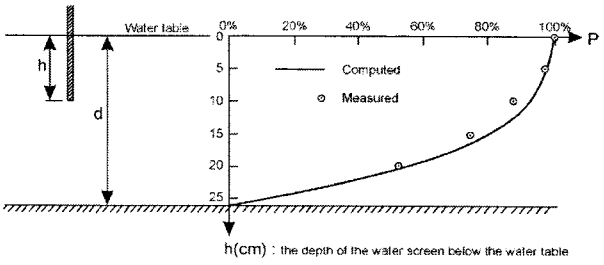

Fig. 11. Transmission ratio of incident wave energy (P) according to the depth of a water screen; total water depth is 26 cm (Bruun 1989).

of the water depth. Hence, wave height at A2 can also be obtained reasonably with the regression formula.

Based on the data, the temporal variation of current-induced and wave-induced bed shear stresses can be calculated by the following equations (van Rijn 1989):

$$\tau_c = \frac{1}{8}\rho f_c U^2 \quad (1)$$

$$\tau_w = 0.25\rho f_w u_w^2 \quad (2)$$

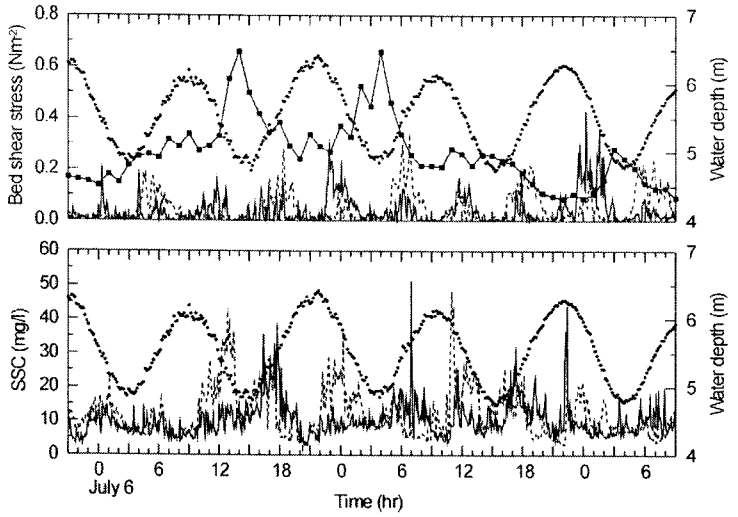

Fig. 12. Temporal variations of wave- and current- induced bed shear stress, water depth and SSC; filled circles of both panels represent water depth at site A1. Solid line with filled square of the upper means τ_w at A1, solid lines represent τ_c, and SSC at A1 and dotted lines those at A2.

where, τ_c is the bed shear stress applying to the bed by depth-mean current (U), and τ_w is period-averaged wave-induced bed stress, ρ is the density of seawater, f_c are f_w are current- and wave-induced bed friction factors, respectively, and u_w is the peak orbital velocity of fluid at the edge of the wave boundary layer. Depth-mean current velocity is calculated by the equation for the universal logarithmic profile. The current-induced bed friction factor is calculated by the equation of van Rijn (1989), in which the zero-velocity level is assigned as 0.05 cm, the average of the values for mud and mud/sand (Soulsby 1983). The wave-induced friction factor is calculated by the equation of Jonsson (1966).

In order to simply understand the relationship between hydrodynamic forcing and SSC response, calculated time series of bed shear stresses are shown with water depth and SSC in Fig. 12. Wave-induced bed shear stress is much higher than τ_c except for the short period, including the maximum τ_c of 0.43 N/m^2 at 00:15 on July 8. The maximum τ_w is 0.66 N/m^2 occurred at 14:00 on July 6 when the significant wave period, water depth, and estimated significant wave height were 13 s, 4.92 m, and 0.41 m, respectively.

It is apparent that SSC peaks are related to the major and sub-major peaks of τ_w. For the two major peaks of τ_w and associated SSC, however, there are two processes to be considered. First, due to the fact high concentrated suspension by wave loading is confined in the near bed region (e.g., Bosman 1982; Mehta 1988), there is no SSC peak at low water even though the τ_w is considerable. Additionally, the SSC at A2 is much higher than that at A1 during the growing-up periods of the two major peaks of τ_w, while that at A1 is slightly higher during the pariods of growing down, although the time lag between the peak values of τ_w of the sites is considered negligible. It may be explained by the mean diameter of bottom sediments. As shown in Table 2, the mean diameter of 62.5 μm at A1 is much coarser than that of 15.6 μm at A2. Hence, it is natural that the SSC at A1 should be much lower. Additionally, SSC increases at A1 during the flood period seem to be largely caused by the advection of the SS entrained in the area of A2.

Estimation of the screen efficiency

The behavior of current speed and SS influenced by the silt screen and waves in the study area are roughly understood as described above. However, the results are not enough to estimate the efficiency of the screen in reducing the dispersion of dredging-induced SS plume because there is no data for the second half period of the AURY monitoring at A1, and current measurements were not concurrently performed with the cruise profiling of the SSC at 6 sites near the screen.

Temporal variations of calculated SS fluxes at 3 mab at A1 and A2 are shown in Fig. 13. Due to no dredging taking place during the storm period and no data at A1 in the latter half of the period, the only possible period for comparing fluxes in the plume SSC generated by dredging

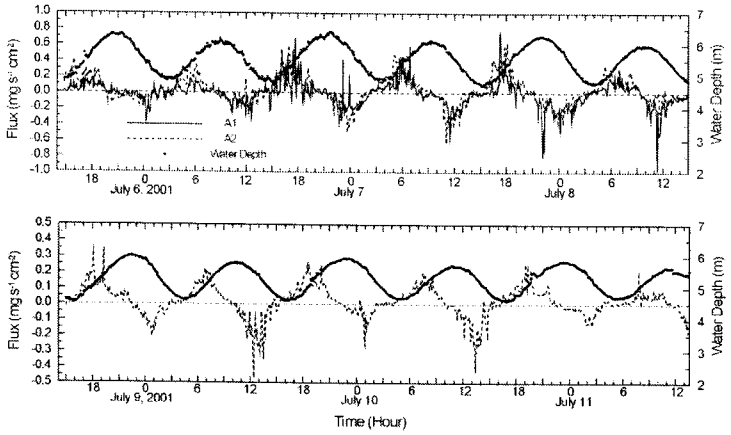

Fig. 13. Temporal variations of SS fluxes at 3 mab of sites A1 and A2 (dotted line).

Table 4. Comparison of SS fluxes per unit area (g s^{-1} cm^{-2}) at 3 mab of sites at A1 and A2 according to dredging conditions.

Period & Site / Flux dir.	w/o Dredging 20:30 07/05-03:30 07/06		Dredging 09:30-15:00 07/08	
	A1	A2	A1	A2
Northward	0.145	0.204	0.000	0.013
Southward	1.342	1.276	2.885	1.297
Net	1.197	1.072	2.885	1.284

is during the second ebb period on July 6 when all the 3 dredgers were working. It may be useful to compare them with the fluxes during the ebb period of mild sea conditions without dredging. Table 4 shows that the southward net fluxes during the normal ebb period are comparable between the two sites, while the flux of A2 is lower than that of A1 by 55.5% during the dredging period.

However, it is the efficiency only that is considered at the mid-depth. Considering the SSC profiles showing much higher SSC at A2 in Fig. 7, the SSC fluxes at the two sites may be comparable.

5. Conclusions

Hydrodynamic measurements in a microtidal coastal area near Busan New Port, lead to a few of the preliminary conclusions in association with the installation of silt screens and working of dredgers:

1) Current speed at about 30 m downstream of the silt screen of which the vertical length is the half of the total water depth, is about half that found at the same distance upstream.

2) Vertical gradient of the current velocity upstream of the screen is steeper than downstream.

3) Even for a relatively weak storm period, SSC increases up to the value caused by dredging.

4) Depth-averaged SSC downstream of the screen is higher by 60% than upstream, contrary to the major purpose of the screen, which is to reduce SSC.

5) Screen efficiency evaluated by the SSC flux at the mid-layer is about 55%. Considering the higher SSC downstream, however, depth-integrated flux downstream may be comparable to that upstream.

6) Considering the above results, the silt screen of the fixed hanging type installed from the surface to about the half of the water depth does not confirm a mitigation measure against the spreading of the SS plumes generated by dredging in the study area where the mean current velocity ranges about 20 to 30 cm/s.

Acknowledgements

This study was supported by the Ministry of Maritime Affairs and Fisheries under grant numbers PM01113 and PM01117. The authors are grateful to Mr. W. D. Baek and Mr. Y.C. Kim of KORDI for their devotional contribution to the field measurements and laboratory experiments. Thanks are extented to Drs. Hee Jun Lee and Hyoseob Kim for their constructive comments on this manuscript.

References

Bosman, J. 1982. Concentration measurements under oscillatory motion. Report M1695-II, Delft Hydraulics, Delft, The Netherlands.

Bruun, P. 1989. Port Engineering. 4th ed. Gulf Pub. Co.

D&A Instrument Company. 1991. Instruction manual OBS-1 & 3.

Jin, J.-Y., K.C. Hwang, J.S. Park, K.S. Lee, K.D. Yum, and J.K. Oh. 2003. Development of a programmable suspension sampler to improve the monitoring of sediment-transport processes. In: *Proc. (CD) Coastal Sediment '03,* Clearwater Beach, FL, USA.

Jonsson, I.G. 1966. Wave boundary layer and friction factors. p. 127-148. In: *Proc. 10th Conf. Coastal Eng.*

KORDI. 2000. Restoration of the eastern marginal environment of the Yellow Sea (REYES) : Creation and restoration of environmentally sustainable tidalflat. (CREST) BSPE 00785-00-112-2. (In Korean with English summary)

KORDI. 2001. Maintenance of a directional wave rider for breakwater construction of Busan New Port. BSPI 329-00-1362-2. (In Korean)

Mehta, A.J. 1988. Laboratory studies on cohesive sediment deposition and erosion. In: *Physical Processes in Estuaries,* ed. by J. Dronkers and W. van Leussen. Springer-Verlag, Berlin, Germany.

Mouchel Asia Ltd. 2002. Infrastructure for Penny's Bay Development-Contract 1/Quarterly environmental monitoring and Audit (EM&A) Report (No.2) March 2002-May 2002-Rivision A.

Ooms, K. 1997. Disposal and capping of contaminated sediments - the Hong Kong solution. In: *Proc. the CEDA Dredging Days*, Amsterdam, The Netherlands.

Reine, K.J., D.D. Dickerson, and D.G. Clarke. 1998. Environmental windows associated with dredging operation. *Technical Note, DOER-E2.* U.S. Army Engineer Research and Development Center, Vicksburg, MS.

Soulsby, R.L. 1983. The bottom boundary layer of shelf seas. In: *Physical Oceanography of Coastal and Shelf Sea*, ed. by B. Johns. Elsevier Science Pub., Amsterdam, The Netherlands.

van Rijn, L.C. 1989. Handbook of sediment transport by currents and waves. Report H461, Delft Hydraulics, Delft, The Netherlands.

Received Jul 5, 2003
Revised Oct. 1, 2003
Accepted Nov. 27, 2003